Capsule-Type Magnetic Microrobot Actuated by an External Magnetic Field for Selective Drug Delivery in Human Blood Vessels

Kyun Choi, Gunhee Jang, Seungmun Jeon, and Jaekwang Nam

Precision Rotating Electromagnetic Machine Laboratory, Department of Mechanical Engineering, Hanyang University, Seoul 133-791, Korea

In this paper, we propose a novel capsule-type magnetic microrobot (CMM) that can navigate along a tubular environment and selectively release drugs in different target points actuated by a magnetic navigation system. The proposed CMM is a capsule-type structure with two cylindrical drug chambers that contain different drugs. It can navigate through a tubular environment by a magnetic gradient and release drugs at different positions by using uniform rotating magnetic fields. The proposed CMM was prototyped using 3-D printing technology. The operating conditions of a drug-releasing motion were determined by investigating the magnetic and friction torques within the body. Finally, we performed various experiments in a tubular environment to verify the validity of the proposed CMM.

Index Terms—**Magnetic microrobot, magnetic navigation system, rotating screw motion, targeted drug delivery.**

I. Introduction

VASCULAR diseases, such as hardening of the arteries and angina pectoris, are one of the leading causes of human death in modern society [1], [2]. One of the conventional treatments is to use a catheter composed of a flexible tube and wire to unclog the diseased blood vessels [1]. Although it is a simple surgery, the success of catheterization is mainly dependent on the maneuverability of the catheter and the experience of the medical doctors. Magnetic microrobots manipulated by a magnetic navigation system (MNS) have been widely investigated as a possible alternative to conventional treatments. This method is a minimally invasive but highly efficient treatment compared with conventional treatments. One part of the microrobot is composed of a permanent magnet, and the coil system of the MNS generates a uniform or gradient magnetic field to control the motion of the microrobot located inside of the MNS [3], [4].

Several researchers have developed various mechanisms for microrobots [5], [6]. Pan *et al*. [7] proposed a spiral-type robot operated by a rotating magnetic field that generates thrust force to move the robot to the target position within a fluid. Nam *et al.* [8] developed a crawling-type robot with flexible legs that generates an asymmetric friction force originating from an oscillating magnetic field to move along a tubular environment. However, the objective of these robots was limited to moving in various environments, and they could not perform therapeutic functions, such as drug delivery. Kim and Ishiyama [9] developed a spiral-type robot for drug release that utilizes thrust forces with opposite directions through two mechanically connected spiral bodies. However, it was difficult to apply their robot to the blood vessels of variable diameters since the motion of their robot utilizes wall friction.

Manuscript received March 7, 2014; revised April 18, 2014; accepted May 6, 2014. Date of current version November 18, 2014. Corresponding author: G. Jang (e-mail: ghjang@hanyang.ac.kr).

Color versions of one or more of the figures in this paper are available online at http://ieeexplore.ieee.org.

Digital Object Identifier 10.1109/TMAG.2014.2325055

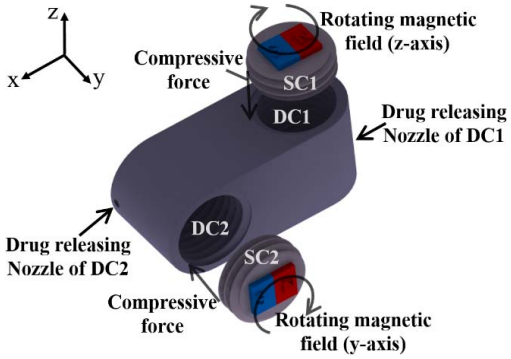

Fig. 1. Mechanical structure of the proposed CMM.

We propose a novel CMM that can navigate along tubular environment and selectively release the drug in different target points by an MNS. The proposed CMM is a capsule-type structure, as shown in Fig. 1, and it is composed of two cylindrical drug chambers (DC1 and DC2) that can contain different drugs. Each chamber has tapped holes along the central axis (DC1: z-axis, DC2: y-axis) and it is covered by screw caps (SC1 and SC2). The permanent magnets are inserted into SC1 and SC2. DC1 and DC2 also have independent drug releasing holes, so that each screw motion of SC1 and SC2 can selectively release a drug from DC1 and DC2. We determine the operating conditions of the drug-releasing motion by investigating the magnetic and friction torques. We finally perform various experiments in a tubular environment to verify the validity of the proposed CMM.

II. Operation of the CMM

A. Aligning and Linear Propelling Motion of the CMM

The motion of the proposed CMM is composed of an aligning motion that determines the moving direction, a linear propelling motion that moves back and forth along the aligned direction, and a rotating screw motion that releases the drug.

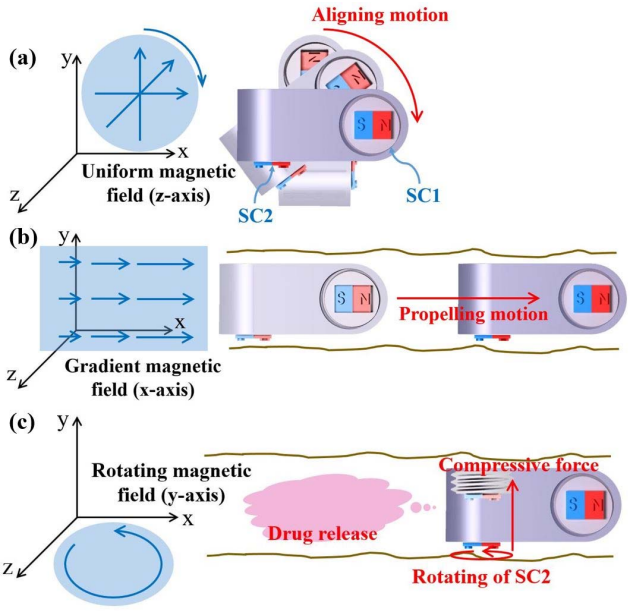

Fig. 2. (a) Aligning motion of the CMM. (b) Linear propelling motion of the CMM. (c) Rotating screw motion of the CMM.

It is controlled by the magnetic torque and force, which can be expressed as follows:

$$\mathbf{T} = V\mathbf{M} \times \mathbf{B} \tag{1}$$

$$\mathbf{F} = V(\mathbf{M} \cdot \nabla)\mathbf{B} \tag{2}$$

where V, $\mathbf{M}$, and $\mathbf{B}$ are the volume, the magnetization of the microrobot, and the applied magnetic flux density, respectively. The CMM is driven by the MNS which generates and controls the magnetic gradient and the uniform magnetic field from its coil system to generate the magnetic torque and force. Fig. 2 shows the aligning, linear propelling, and rotating screw motions of the CMM. From (1), the uniform magnetic field generates the magnetic torque to align the CMM along the same direction as the external magnetic field. Assuming that the CMM is initially placed on the xy-plane, the z-directional uniform rotating magnetic field can synchronously turn the CMM to the clockwise direction, as shown in Fig. 2(a). Once the directions of the magnets in SC1 and SC2 are aligned toward the target point through this aligning motion, the x-directional magnetic gradient is applied to the CMM so that the CMM moves to the x-direction, as shown in Fig. 2(b). To move the CMM in the opposite direction, SC1 and SC2 are rotated 180° or the negative magnetic gradient is applied.

B. Rotating Screw Motion and Drug Release

Rotating the uniform magnetic field generates the rotating screw motion of the screw cap to release the drug in the drug chamber by compressive force, as shown in Fig. 2(c). The rotating magnetic field can be expressed as follows:

$$\mathbf{B}_{\text{rmf}}(t) = B_0(\cos\omega t\mathbf{U} + \sin\omega t\mathbf{N} \times \mathbf{U}) \tag{3}$$

where B_0, ω, $\mathbf{N}$, and $\mathbf{U}$ are the magnitude and angular velocity of the rotating magnetic field, the unit vector of the rotating axis, and the unit vector normal to $\mathbf{N}$, respectively. The magnetic torque applied to the CMM can be calculated by substituting (3) into (1). A drug can be selectively released by coinciding the direction of $\vec{N}$ with the rotating axis of the screw cap, as shown in Fig. 3. For example, if the CMM is aligned in the x-direction within a narrow passage as shown in Fig. 2(c), a clockwise rotating magnetic field (y-axis) on the xz-plane is required to release the drug in SC2.

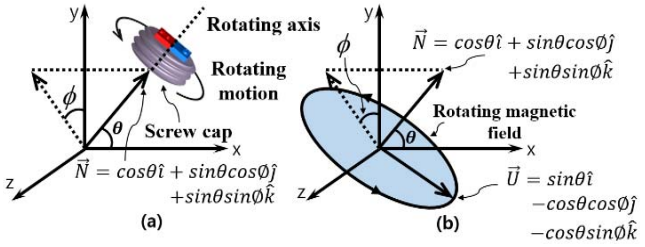

Fig. 3. (a) 3-D rotating motion of the screw cap. (b) Rotating magnetic field required to generate the rotating motion of the screw cap.

The operating condition to release the drug is determined by analyzing the magnetic torque and force applied to the CMM. The permanent magnets in SC1 and SC2 exert magnetic force and torque as follows:

$$\mathbf{F}_m = \frac{3\mu_0}{4\pi r^5}\left[(\mathbf{m}_1 \cdot \mathbf{r})\mathbf{m}_2 + (\mathbf{m}_2 \cdot \mathbf{r})\mathbf{m}_1 + (\mathbf{m}_1 \cdot \mathbf{m}_2)\mathbf{r} - \frac{5(\mathbf{m}_1 \cdot \mathbf{r})(\mathbf{m}_2 \cdot \mathbf{r})}{r^2}\mathbf{r}\right] \tag{4}$$

$$\mathbf{T}_m = \mathbf{m}_2 \times \frac{\mu_0}{4\pi}\left[\frac{3\mathbf{r}(\mathbf{m}_1 \cdot \mathbf{r})}{r^5} - \frac{\mathbf{m}_1}{r^3}\right] \tag{5}$$

where $\mu_0, \mathbf{r}, \mathbf{m}_1$, and $\mathbf{m}_2$ are the permeability of the air, distance between the permanent magnets in SC1 and SC2, and magnetization of the permanent magnets in SC1 and SC2, respectively.

To release the drug from DC2, the external magnetic torque applied to SC2 ($\mathbf{T}_{\text{ext}}$) should be greater than the resisting torque, which is the summation of the magnetic torque generated by the interaction between the permanent magnets in SC1 and SC2 ($\mathbf{T}_m$), the friction torque generated by the screw motion between SC2 and DC2 ($\mathbf{T}_f$), and the friction torque by the attractive force between the permanent magnets in SC1 and SC2 ($\mathbf{T}_{\text{att}}$). The operating condition of the CMM to release a drug can be expressed as follows:

$$\mathbf{T}_{\text{ext}} > \mathbf{T}_m + \mathbf{T}_f + \mathbf{T}_{\text{att}} \tag{6}$$

$$\mathbf{T}_{\text{att}} = \mu\mathbf{F}_m \times r. \tag{7}$$

III. Results and Discussion

A. Prototyped CMM and MNS

As shown in Fig. 4, the proposed CMM was prototyped by using 3-D printing technology. The width, height, and length of the CMM were 6.5, 6.5, and 14 mm, respectively. The ∇ volume of each chamber was 61.5 mm^3, and seven rotating screw motions released all the drug filled in the chamber. Cylindrical neodymium magnets with a diameter of

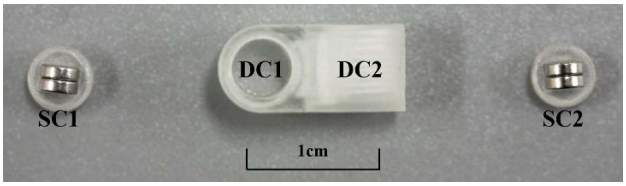

Fig. 4. Prototyped CMM.

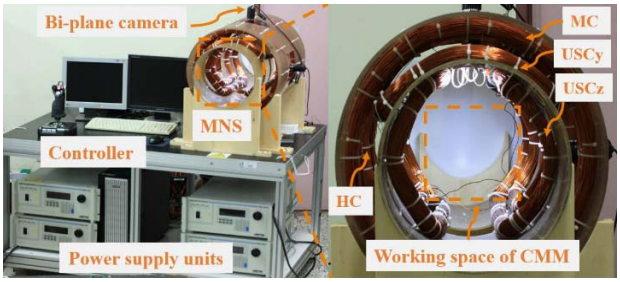

Fig. 5. MNS to generate and control an external magnetic field.

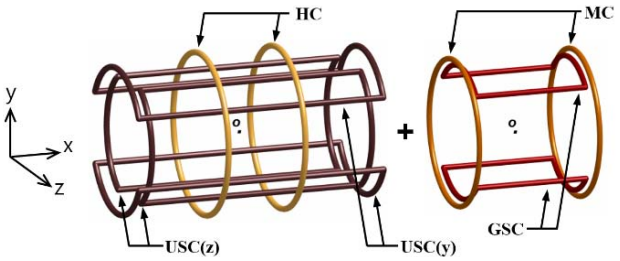

Fig. 6. Coil system in the MNS.

TABLE I
MAJOR SPECIFICATIONS OF THE MNS

Coil	Radius (mm)	Wire diameter (mm)	Coilturns
HC	216.0	1.0	430
USC(y)	167.5	1.2	400
USC(z)	133.8	1.2	320
MC	216.0	1.3	920
GSC	138.5	1.0	300

3 mm, a length of 2 mm, and magnetization of 955 kA/m were inserted into SC1 and SC2.

We constructed an MNS to operate the CMM, as shown in Fig. 5 [4]. A major component of the MNS is the coil system as shown in Fig. 6, which was configured with a Maxwell coil (MC), Helmholtz coil (HC), gradient saddle coil (GSC), and two uniform saddle coils (USCs). The MC and the GSC generate the magnetic gradient while the HC and the USCs generate the uniform magnetic field [4]. The major specifications of the MNS are shown in Table I. The MNS with four coils [MC, GSC, HC, and USC(y)] can move the CMM by selectively generating the magnetic gradient and the uniform magnetic field in 2-D plane, and the MNS with three coils [HC, USC(y), and USC(z)] can release the drug by the rotating magnetic field in 3-D space. Table II shows the maximum voltage, current, magnetic flux density, magnetic gradient, and the corresponding torque and force in the developed MNS. The HC and the USCs generate a maximum uniform magnetic field of 14.04 mT. A watery tubular environment was constructed inside the MNS to perform the drug-releasing experiment of the CMM.

TABLE II
MAXIMUM VOLTAGE, CURRENT, MAGNETIC FLUX DENSITY AND GRADIENT, AND MAGNETIC TORQUE AND FORCE IN THE DEVELOPED MNS

	Coil	V[V]	I[A]	B / ∇B	Torque / Force
Uniform	HC	200.0	7.78	14.04[mT]	192mN·mm
	USC(y)	115.2	7.63		
	USC(z)	251.2	7.8		
Gradient	MC	275.2	7.63	121.25[mT/m]	2.8mN
	GSC	162.0	12.96	83.83[mT/m]	

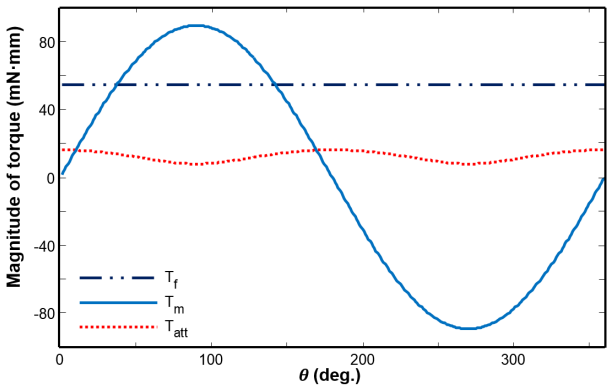

Fig. 7. Resisting torques exerted on the SC2: magnetic torque exerted on the SC2 due to the permanent magnet in the SC1 ($\mathbf{T}_m$), friction torque exerted on the SC2 due to the attractive force between the permanent magnets ($\mathbf{T}_{\text{att}}$), and friction torque exerted on the SC2 due to the screw motion $\mathbf{T}_f$.

B. Analysis of the Screw Motion of the CMM

Fig. 7 shows the resisting torques exerted on the SC2 due to the angular difference of the magnetization direction between the permanent magnets in the SC1 and SC2. Equation (5) can calculate the magnetic torque exerted on the SC2 ($\mathbf{T}_m$) generated by the interaction between the permanent magnets in SC1 and SC2, whose maximum and minimum values are 89 mN·mm at 90° and 0 mN·mm at 0°, respectively. The friction torque of the SC2 ($\mathbf{T}_f$) can be calculated by (1) once the minimum magnetic flux density to begin the screw motion between SC2 and DC2 is measured. The external magnetic field for the CMM without SC1 increases gradually to determine the minimum magnetic flux density to begin the screw motion between SC2 and DC2, and it is 4 mT. The corresponding magnetic torque of 55 mN·mm is calculated from (1). Also, the external magnetic field for the CMM with both SC1 and SC2 increases gradually to determine the minimum magnetic flux density to start the screw motion between SC2 and DC2, and it is 11.2 mT. The minimum magnetic torque ($\mathbf{T}_{\text{ext}}$) to generate the screw motion between SC2 and DC2, including the interaction between magnets, is 160 mN·mm. We have $\mathbf{T}_m$, $\mathbf{T}_f$, and $\mathbf{T}_{\text{ext}}$ in (6), and the attractive force ($\mathbf{F}_m$) between the permanent magnets in SC1 and SC2 can be calculated from (4). From (7), the friction coefficient of 0.3 is calculated due to the screw motion between SC2 and DC2. As shown in Table II, the HC and the USCs generate the maximum uniform magnetic field of 14.04 mT. The maximum

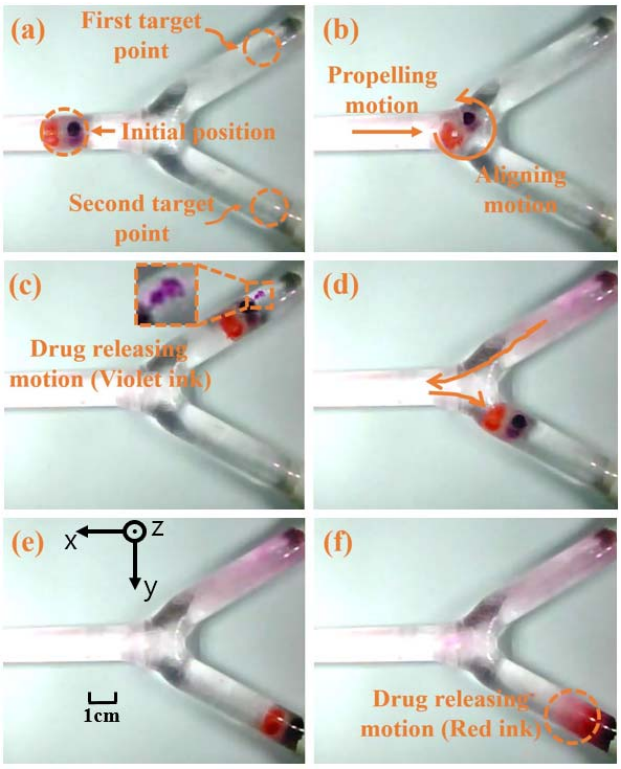

Fig. 8. Navigating and drug-releasing experiment of the CMM in a narrow tubular environment. (a) Initial position of the CMM. (b) Propelling and aligning motions of the CMM. (c) Drug-releasing motion (violet ink) of the CMM. (d) Backward propelling motion and aligning motion of the CMM toward the second target point. (e) Propelling motion to reach the second target point. (f) Drug-releasing motion (red ink) of the CMM.

magnetic torque of 192 mN·mm was calculated from (1). The minimum external magnetic flux density to operate the CMM is 11.2 mT, and if the magnitude of the external magnetic field is smaller than 11.2 mT, the proposed CMM cannot release the drug in the given experiment.

C. Targeted Drug Delivery of the CMM

We finally performed the experiment of the targeted drug delivery of the CMM in a watery y-shaped tubular environment to verify the validity of the proposed CMM, as shown in Fig. 8. Fig. 8(a) shows the x-directional propelling motion generated from the x-directional magnetic gradient once the permanent magnets in SC1 and SC2 were aligned along the x-direction, and the CMM reached a bifurcated position. Fig. 8(b) shows that the z-directional uniform magnetic field rotated the CMM counterclockwise in order to align toward the first target point. The magnetic gradient was applied to generate a linear propelling magnetic force toward the first target point, and the prototyped CMM reached the first target point. To release the drug from DC1, the MNS generated a uniform magnetic field in the same direction as the axial direction of SC1 and with the rotating frequency of 0.1 Hz. This was applied to screw down SC1 and release the drug (violet ink) from DC1 at the first target point, as shown in Fig. 8(c). Fig. 8(d) shows that the prototyped CMM moved back to the bifurcated position with the application of the magnetic gradient from the opposite direction and that the z-directional uniform magnetic field rotating in the clockwise direction was applied to the CMM in order to align toward the second target point. Fig. 8(e) shows that the magnetic gradient was applied the CMM to generate a linear propelling magnetic force to reach the second target point. Finally, Fig. 8(f) shows that the uniform rotating magnetic field with the same direction as the axial direction of SC2 and a rotating frequency of 0.1 Hz was applied the CMM to screw down SC2 and release the drug (red ink) in DC2 at the second target point. This experiment demonstrates the possibility that the proposed CMM could precisely and selectively deliver different drugs to multiple targets in human blood vessels.

IV. Conclusion

We proposed a novel CMM that can navigate along tubular environment and selectively release the drug in target point by an MNS. We determined the operating conditions of the drug-releasing motion by investigating the magnetic and friction torques mathematically and experimentally. We finally performed various experiments in a tubular environment to verify the validity of the proposed CMM. This paper could contribute to the development of a microrobot with multi-functions to treat human coronary artery diseases efficiently.

Acknowledgment

This work was supported by the National Research Foundation of Korea through the Korean Government under Grant 2012R1A2A1A01.

References

[1] *Heart Disease and Stroke Statics*, American Heart Association & American Stroke Association, Dallas, TX, USA, 2013.

[2] P. B. Shah, "Management of coronary chronic total occlusion," *Circulation*, vol. 123, no. 16, pp. 1780–1784, 2011.

[3] S. M. Jeon, G. H. Jang, H. C. Choi, S. H. Park, and J. O. Park, "Magnetic navigation system for the precise helical and translational motions of a microrobot in human blood vessels," *J. Appl. Phys.*, vol. 111, no. 7, pp. 07E702-1–07E702-3, Apr. 2012.

[4] S. M. Jeon, G. H. Jang, H. C. Choi, and S. H. Park, "Magnetic navigation system with gradient and uniform saddle coils for the wireless manipulation of micro-robots in human blood vessels," *IEEE Trans. Magn.*, vol. 46, no. 6, pp. 1943–1946, Jun. 2010.

[5] H. Zhou, G. Alici, T. D. Than, and W. Li, "Modeling and experimental characterization of propulsion of a spiral-type microrobot for medical use in gastrointestinal tract," *IEEE Trans. Biomed. Eng.*, vol. 60, no. 6, pp. 1751–1759, Jun. 2013.

[6] S. H. Kim, K. Shin, S. Hashi, and K. Ishiyama, "Magnetic fish-robot based on multi-motion control of a flexible magnetic actuator," *Bioinspiration Biomimet.*, vol. 7, no. 3, p. 036007, 2012.

[7] Q. Pan, S. Guo, and D. Li, "Mechanism and control of a spiral type of microrobot in pipe," in *Proc. IEEE Int. Conf. ROBIO*, Feb. 2009, pp. 43–48.

[8] J. K. Nam, G. H. Jang, S. M. Jeon, and S. J. Kim, "Crawling microrobot actuated by a magnetic navigation system in tubular environments," *Sensors Actuat. A: Phys.*, vol. 209, pp. 100–106, Mar. 2014.

[9] S. H. Kim and K. Ishiyama, "Magnetic robot and manipulation for active-locomotion with targeted drug release," *IEEE/ASME Trans. Mechatronics*, vol. 19, no. 5, pp. 1651–1659, Oct. 2014.